Facile Synthesis and Properties of Hierarchical Double-Walled Copper Silicate Hollow Nanofibers Assembled by Nanotubes

Renxi Jin,[†] Yang Yang,[†] Yan Xing,[†,*] Li Chen,[†] Shuyan Song,[‡,*] and Rongchao Jin[§]

[†]Department of Chemistry, Northeast Normal University, Changchun, 130024, People's Republic of China, [‡]State Key Laboratory of Rare Earth Resource Utilization, Changchun Institute of Applied Chemistry, Chinese Academy of Sciences, Changchun, 130022, People's Republic of China, and [§]Department of Chemistry, Carnegie Mellon University, Pittsburgh, Pennsylvania 15213, United States

ABSTRACT

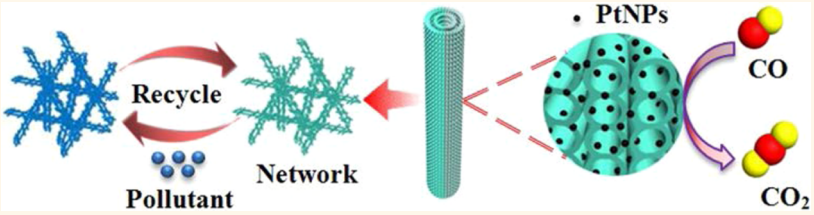

The hierarchical assembly of multilevel, nonspherical hollow structures remains a considerable challenge. Here, we report a facile approach for synthesizing copper silicate hollow nanofibers with an ultrasmall nanotube-assembled, double-walled structure. The as-prepared hollow fibers possess a tailored complex wall structure, high length-to-diameter ratio, good structural stability, and a high surface area, and they exhibit excellent performance as an easily recycled adsorbent for wastewater treatment and as an ideal support for noble metal catalysts. In addition, this strategy can be extended as a general approach to prepare other double-walled, hollow, fibrous silica-templated materials.

KEYWORDS: hollow nanofibers · nanotubes · silicates · wastewater treatment · supported catalysis

With the advances in materials science, much emphasis has been placed on hollow micro/nanomaterials owing to their promising applications, such as catalysis, nanoreactors, gas sensors, energy storage and conversion, and biomedical engineering.[1−4] As a special branch of micro/nanomaterials, one-dimensional (1D) hollow nanomaterials, including nanotubes and hollow nanofibers, have been extensively pursued in recent years, for their unique one-dimensional structure and high surface area, which provide many novel properties and functionalities.[5−10] Several methodologies have been demonstrated for processing a broad range of materials into 1D hollow micro/nanomaterials; however, the resulting nanostructures are mostly composed of single-layer wall structures. To meet the emerging needs of multifunctional and integrative devices, hollow micro/nanomaterials with more complex inner structures are urgently needed. More recently, multilevel 1D hollow architectures with higher order structuring, including fiber-in-tube, tube-in-tube, multiwalled, and multichannel hollow fibers, have received more attention because of their improved properties compared to those of the simple hollow structures.[11−15] The complex interior structures and multiphase interfaces enable one to better control the local chemical microenvironment and multiple interface reactions for novel physicochemical properties. Additionally, multilevel hollow architectures are considerably more robust than single-wall structures because of the synergistic effect of the two walls that toughens the shell.[16−18] Some ingenious approaches, including the galvanic replacement reaction,[19,20] the Kirkendall effect,[21] nonequilibrium heat

* Address correspondence to xingy202@nenu.edu.cn; songsy@ciac.ac.cn.

Received for review January 15, 2014 and accepted March 11, 2014.

Published online March 11, 2014
10.1021/nn500275d

treatment,[22,23] the template method,[24,25] and multifluidic compound-jet electrospinning techniques,[26,27] have been developed for synthesizing hollow fibers/tubes with multilevel interior structures. However, the walls of most of these multilevel structures are generally composed of or aggregated from nanoparticles with an irregular arrangement, which limits the advancement of their performance.

Hierarchical self-assembly of nanoscale building blocks (clusters, wires, belts, sheets, tubes, *etc.*) into novel architectures of higher dimensionality can help to enhance properties by avoiding aggregation while maintaining the high specific surface areas.[28−33] The combination of hierarchical nanoarchitectures with multilevel hollow 1D micro/nanostructures to form hollow fibers/tubes with hierarchical wall structures represents a promising type of nanomaterial. The more complex wall structures may cause the multilevel hollow fibers to have higher specific surface areas, more active sites, better mechanical strength properties, and enhanced permeability. However, reports on the preparation of multilevel hollow fibers with hierarchical walls constructed from anisotropic building blocks are relatively scarce, partly because of the difficulty in controlling the assembly of primary building units into hierarchical structures to form tube-in-tube structures. Therefore, developing a new strategy for fabricating hollow fibers with multiwall and especially complex wall structures remains a major challenge.

Herein, we demonstrate a facile route for fabricating copper silicate hierarchical double-walled hollow nanofibers by combining the electrospinning technique with the hydrothermal method. To the best of our knowledge, this is the first report on synthesizing unique 1D hollow nanofibers with double walls constructed from 1D ultrasmall nanotubes. As illustrated in Scheme 1, uniform silica hollow nanofibers (SHNFs) prepared using a facile single-capillary electrospinning method are employed as the precursor. Then, double-walled copper silicate hollow nanofibers (CSHNFs) are synthesized using a simple hydrothermal treatment in an alkaline solution based on an SHNF sacrificial templating process. During the hydrothermal process, the SiO_2 wall provides two interfaces for nucleation and a discrete space for simultaneous self-assembled nanotube growth along opposite directions, and it acts as the *in situ* template for the second cavity. Through this method, hollow 1D nanostructures with nanotube-assembled double walls are formed and connected with each other to produce a network structure. The high length-to-diameter ratio of the nanofibers allows for convenient separation and recycling by sedimentation. The designed double-walled CSHNFs possess a tailored complex wall structure, good structural stability, and a high surface area, and they exhibit excellent performance in wastewater treatment as a remarkable adsorbent and as a good support for noble metal catalysts. More importantly, the synthetic strategy developed in this work can be extended to fabricate other double-walled hollow nanofibrous silica-templated materials, making the strategy useful and widely applicable for preparing advanced silicate materials.

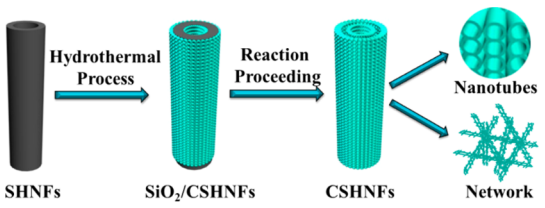

Scheme 1. Formation process of hierarchical double-walled copper silicate hollow nanofibers.

RESULTS AND DISCUSSION

Synthesis and Characterization of Hierarchical Double-Walled CSHNFs. SHNFs were prepared *via* a facile single-capillary electrospinning technique followed by calcination at 550 °C. As shown in Figures 1a and S1a, the electrospun SiO_2 nanofibers align in random orientations and interweave to form a nonwoven fibrous film. The fibers have nearly uniform diameters (200−400 nm) with extremely long lengths and are connected to form a network structure. The corresponding TEM image in Figure 1b indicates that the SiO_2 nanofibers have a typical hollow structure with a wall thickness of approximately 60 nm. Moreover, the surface of the hollow nanofibers is relatively smooth because of the amorphous nature of silica. After hydrothermal treatment in an alkaline solution containing copper ions at 140 °C for 10 h, the as-fabricated sample

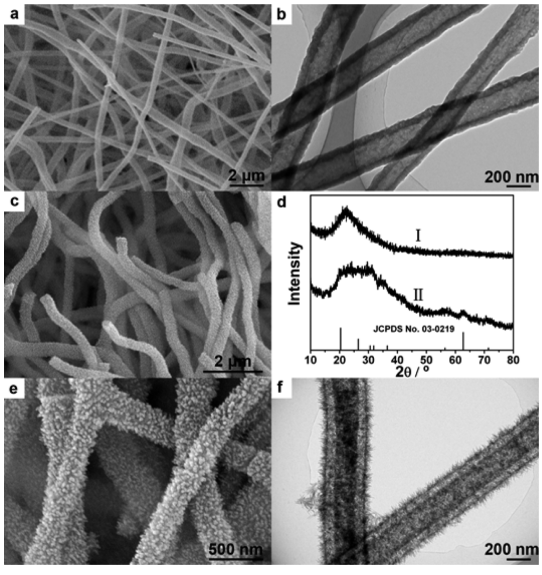

Figure 1. Typical FESEM (a) and TEM (b) images of SiO_2 hollow nanofibers; low-magnification SEM image (c) of CSHNFs; XRD patterns (d) of the two samples: (I) SHNFs and (II) CSHNFs; high-magnification FESEM (e) and TEM (f) images of CSHNFs.

retains its nonwoven fibrous morphology, while the diameters of these fibers are further increased to 300−500 nm, as shown in Figures 1c and S1b. Additionally, the surface of the hollow fibers is no longer smooth. The phase compositions and phase structures of the samples were examined by powder X-ray diffraction (XRD). For silica hollow fibers, the broad band located at $2\theta = 22°$ can be assigned to the characteristic diffraction peak of amorphous SiO_2 (Figure 1d, profile I). After the hydrothermal treatment, the XRD pattern of the obtained fibers shows characteristic broad diffraction peaks that can be indexed to copper silicate ($CuSiO_3 \cdot 2H_2O$, JCPDS card no. 03-0219) (Figure 1d, profile II).[34] A magnified FESEM image (Figure 1e) clearly reveals that the as-prepared copper silicates based on an SHNF sacrificial templating method appear as 1D hierarchical fibers with a high length-to-diameter ratio and a "hairy" structure along the longitudinal axis of the nanofibers. TEM observation (Figure 1f) indicates that the nanofibers possess a unique double-walled hollow structure, in which clear gaps between the outer and inner walls can be observed. The width of the gaps is approximately 60 nm, which agrees well with the wall thickness of hollow SiO_2 nanofibers. Figure S2 shows the EDX analysis of the as-prepared CSHNFs, which indicates the presence of Cu, Si, and O, proving the formation of copper silicate. The elemental mapping by EDX analysis confirms the presence of Cu, Si, and O homogeneously in the hollow nanofibers (Figure S3).

The microstructure of these nanofibers was further investigated using high-magnification TEM images (Figure 2). As shown in Figure 2a, two walls of CSHNFs are constructed from numerous nanotubes with a narrow size distribution. Many holes can be observed on the surface because of the open ends of the nanotubes being parallel to the electron beam. A magnified image of the holes with black edges and white centers is shown in Figure 2b. The outer and inner diameters of these holes are estimated to be approximately 7.4 and 3.2 nm, respectively. The magnified image of the nanotubes on the walls (Figure 2c) exhibits two parallel dark lines and a darkish center, which also clearly indicates that the building units of the walls are nanotubes with lengths of approximately 70−90 nm. Figure S4 displays the N_2 adsorption−desorption isotherm and the corresponding pore size distribution curve (inset of Figure S4) for the as-prepared CSHNFs. The pore size distribution calculated from the adsorption branch centers at 3.4 nm, which is close to the value determined from the TEM image. The BET surface area is 541.1 m^2/g, and the total pore volume is 1.04 cm^3/g. The 1D nanofibrous morphology, high length-to-diameter ratio, unique hierarchical double-walled hollow structure, small tubular unit, high surface area, and narrow pore size distribution combine to enhance the potential applications for the CSHNFs.

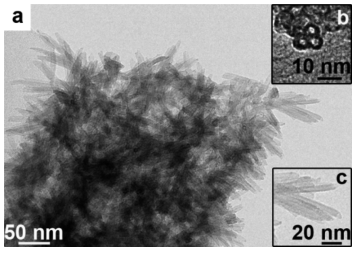

Figure 2. High-magnification TEM images of (a) CSHNFs; (b) holes on the surface of walls; (c) small nanotubes.

Wastewater Treatment. Water pollution is a serious environmental problem in the current society. The utilization of nanostructured silicates in the treatment of organic pollutants in water is of perennial interest because of their low-cost and environmental friendliness.[35,36] However, a potential disadvantage of these nanomaterials lies in that they are easily suspended and difficult to remove from water for recycling of adsorbents, which limits their practical application in wastewater treatment. Inspired by the easy sedimentation of 1D electrospun nanofibers, the as-prepared CSHNFs were investigated as an efficient adsorbent for organic pollutants in wastewater treatment.[37,38] The adsorption isotherm was obtained by varying the initial concentration of solution of methylene blue (MB, as a model organic pollutant in the adsorption experiments) without any additives (Figure S5a). The adsorption isotherm (Figure 3, curve a) indicates that 1 g of newly as-prepared CSHNFs can remove 175 mg g^{-1} of MB, which is higher than that of natural sepiolite (58 mg g^{-1}) and copper silicate hierarchical hollow spheres (162 mg g^{-1}),[34,39] indicating a better adsorption performance of CSHNFs.

A good adsorbent should not only have a high adsorption capacity but also exhibit good regeneration ability for multiple uses. Consequently, two factors need to be considered. First, the stability of the adsorbent to maintain its high adsorption capacity over time must be determined. To test the stability of the

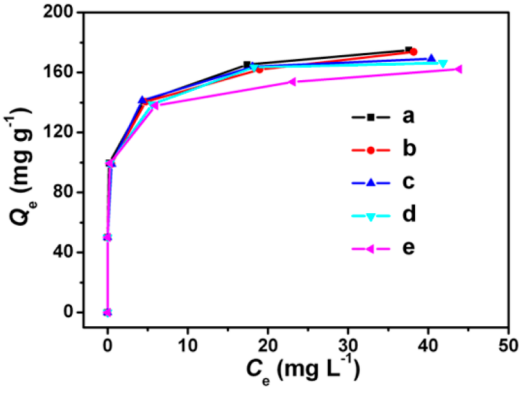

Figure 3. Adsorption isotherm of MB on (a) the newly prepared CSHNFs and those that have been renewed (b) one, (c) two, (d) three, and (e) four times.

CSHNFs, we reused the adsorbent four times. After adsorbing MB, the CSHNFs could be renewed by calcining at 450 °C in air for 2 h. As shown in Figure 3 (curves b−e), the renewed CSHNFs still exhibit good adsorption performance even after running for four cycles. Figure S6 shows that the morphology of the CSHNFs is retained quite well after four cycles of adsorption experiments, which indicates that the CSHNFs have an excellent stability, owing to the synergistic effect of the two walls and the hierarchical structure assembled by nanotubes. Second, the ease with which the adsorbent can be separated from water must also be considered. In this work, the CSHNFs have a fibrous morphology and can be easily separated from an aqueous suspension. As shown in Figure S5b, the CSHNFs are readily deposited to the bottom of vials under gravitation in a short time of only 30 min, likely because of the high length-to-diameter ratio of the 1D hierarchical fibers; in contrast, other morphological silicates have to be separated by centrifugation, by magnetic separation, or by spending several hours or more under gravitational sedimentation.[40−42] The above results show that the as-prepared CSHNFs are a novel material for practical dye removal treatment because of their high adsorption capacity, excellent stability, and ease of sedimentation for separation and reuse.

Catalyst Support. The high specific surface area and excellent stability of the prepared CSHNFs inspire us to further utilize them as a catalyst support for noble metals. Noble metal nanoparticles, especially Pt, have attracted particular interest because of their outstanding catalytic performance in various chemical reactions.[43,44] To achieve Pt-based catalysts with a higher activity and better stability, an efficient method is to disperse well-defined ultrafine Pt nanoparticles onto a suitable support. Herein, we developed a simple and low-energy-consuming approach to deposit and disperse ultrafine Pt nanoparticles on copper silicate hierarchical double-walled hollow nanofibers (PtNPs/CSHNFs). First, the as-prepared CSHNFs with abundant hydroxy groups were activated in a $SnCl_2$ solution.[45] During this process, the Sn^{2+} ion was linked to the CSHNFs surface through inorganic grafting. After chloroplatinic acid ($H_2PtCl_6 \cdot 6H_2O$) was added to the solution at room temperature, the linked Sn^{2+} species acted as a reducing agent to reduce Pt^{4+} *in situ* on the CSHNFs because the standard reduction potential of the Pt^{4+}/Pt redox pair (0.742 V *vs* the standard hydrogen electrode, SHE) is higher than that of Sn^{4+}/Sn^{2+} (0.151 V *vs* SHE).[46] Thus, PtNPs/CSHNFs were successfully obtained.

The as-prepared PtNPs/CSHNFs were imaged by TEM, and the corresponding results are shown in Figure 4. Figure 4a shows that there is essentially no change in the hierarchical double-walled fibrous structure of copper silicate during the growth of PtNPs on its surface. Moreover, it is clearly shown that ultrafine Pt

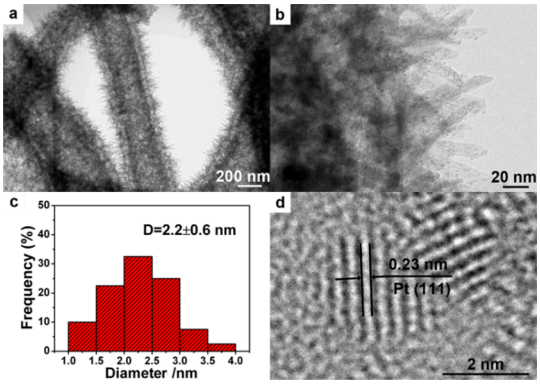

Figure 4. Typical TEM images of the as-prepared PtNPs/CSHNFs (a, b); (c) size distribution histogram of PtNPs; (d) HRTEM image of the PtNPs.

nanoparticles are well dispersed on the surfaces of the small nanotubes (Figure 4b). The size distribution histogram of the PtNPs calculated from the corresponding TEM image is given in Figure 4c. The particle size of Pt is 2.2 ± 0.6 nm. In the HRTEM image (Figure 4d), the interplanar distance of the nanoparticles is 0.23 nm, which agrees well with the lattice spacing of the (111) plane of Pt. The energy-dispersive X-ray (EDX) spectrum from the corresponding TEM image confirms that the above PtNPs/CSHNFs are composed of Cu, Si, O, Sn, and Pt elements (Figure S7). The loading weight of Pt in PtNPs/CSHNFs measured using inductively coupled plasma (ICP) spectroscopy is 1.18 wt %. In addition, the as-prepared PtNPs/CSHNFs were heated at 450 °C for 2 h to investigate their thermal stability. As shown in Figure S8, the Pt particles on the surfaces of the nanotubes maintain their dispersed state without obvious aggregation, which indicates that the PtNPs/CSHNFs have a good thermal stability and resistance to sintering.

High dispersion of ultrafine Pt particles on the CSHNFs can be useful for many potential applications. Here, we selected the gas-phase CO oxidation reaction as a model system to evaluate the catalytic performance of the as-prepared samples. The complete conversion temperature for the as-prepared PtNPs/CSHNFs is 275 °C (Figure 5, curve a). After calcination at 450 °C for 2 h, the complete conversion temperature over the PtNPs/CSHNFs decreases to 190 °C (Figure 5, curve b), which is lower than that of PtNPs/mesoporous silica with various Pt loadings.[47,48] The higher CO oxidation activity of the calcined PtNPs/CSHNFs catalyst may be attributed to an improved crystallization of Pt nanoparticles after calcination. These results confirm that our hierarchical double-walled hollow silicate nanofibers are ideal catalyst supports. The as-prepared PtNPs/CSHNFs are highly active and stable materials for catalytic uses, thus satisfying the requirements for a catalyst for industrial applications.

Importantly, the strategy described above is quite general. We have successfully synthesized other

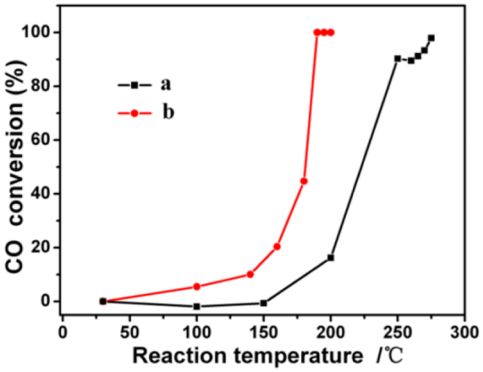

Figure 5. CO oxidation activity of catalysts: (a) PtNPs/CSHNFs; (b) as-prepared PtNPs/CSHNFs after calcination at 450 °C for 2 h.

silicates, such as nickel silicate and magnesium silicate, with hierarchical double-walled hollow fibrous structures using a similar hydrothermal procedure (Figure S9). The TEM image (Figure S9a) shows that the double walls of 1D hollow nickel silicate nanofibers are assembled by thin nanopetals. Magnesium silicate has a similar morphology to nickel silicate, but the building units of the walls are much thinner nanopetals (Figure S9b). These hollow nanofibers with two walls assembled by nanopetals would exhibit better performance than traditional hollow nanomaterials because of the synergistic effect of the robust hierarchical double-wall structure and the flexible nanopetals.

CONCLUSIONS

In summary, we have developed a facile route for fabricating copper silicate double-walled hollow nanofibers assembled by tiny nanotubes. We have also demonstrated the promising use of these interesting hierarchical fibrous structures as adsorbents for wastewater treatment and as supports for noble metal catalysts. Furthermore, this effective strategy is general for the synthesis of other metal silicate materials with hierarchical double-walled hollow nanofibrous morphology. The synthetic strategy holds promise in the preparation of functional, assembled materials. The hierarchical double-walled hollow nanofibers will contribute to environmental remediation and industrial catalysis in the future.

EXPERIMENTAL METHODS

Synthesis of SiO_2 Hollow Nanofibers. SHNFs were prepared through a single capillary electrospinning method. A 0.95 g sample of polyvinylpyrrolidone (PVP) powder (M_n = 90 000) was dissolved in 10 mL of ethanol. Then, 1.6 mL of tetraethyl orthosilicate (TEOS) was slowly dropped into the above PVP solution to obtain the precursor. After that, the precursor was transferred into a plastic syringe for electrospinning under the voltage of 9.5 kV. The products were collected at a distance of about 20 cm to the syringe tip. Finally, the above composites of PVP/TEOS were calcined at a rate of 0.5 °C min^{-1} and remained for 2 h at 550 °C. Thus, SHNFs were obtained.

Synthesis of Hierarchical Double-Walled Copper Silicate Hollow Nanofibers. CSHNFs were prepared through a simple hydrothermal process. In a typical synthesis, copper acetate monohydrate (0.1 mmol), ammonia chloride (2 mmol), and $NH_3 \cdot H_2O$ (0.2 mL, 28%) were added under stirring to 10 mL of distilled water, and the resulting solution and the as-prepared SHNFs (0.01 g) were transferred into a 15 mL Teflon-lined autoclave. The autoclave was sealed and maintained at 140 °C for 10 h. After the autoclave was cooled to room temperature, the resulting light blue precipitates were collected and washed several times with distilled water and absolute ethanol. The final products were dried under vacuum at 60 °C for 4 h. Nickel silicate and magnesium silicate double-walled hollow nanofibers were prepared under a similar experimental process by varying the corresponding acetate and experimental temperature (Ni^{2+}: 100 °C for 10 h; Mg^{2+}: 180 °C for 10 h).

Synthesis of PtNPs/CSHNFs. A 0.01 g amount of $SnCl_2$ was dissolved in 20 mL of HCl (10 mM) solution. Then, 0.01 g of the obtained CSHNFs was added to the above solution and stirred for 2.5 h at room temperature. After this, the precipitates were collected by sedimentation followed by washing with distilled water five times. Thus, the activated CSHNFs were obtained. The activated CSHNFs were mixed with 20 mL of distilled water; then 0.225 mL of H_2PtCl_6 solution (9.4 mM) was added to the above mixture. After stirring for 10 min, PtNPs/CSHNFs were obtained and washed several times with distilled water and absolute ethanol.

Water-Treatment Experiment. Methylene blue solutions were used as the model wastewater for the adsorption of organic pollutants. First, MB solutions with different concentrations of 25, 50, 75, 100, and 125 mg L^{-1} were prepared. The as-obtained CSHNFs (0.01 g) were mixed with 20 mL of the above MB solution, and then the mixed solution was stirred for 10 min and left for a specified time (30 min) until the solid and liquid separated naturally under gravitation. A UV–vis spectrophotometer was used to determine the concentration of MB solution. The adsorption isotherm of MB was obtained by standard spectrophotometric methods at λ = 664 nm. The adsorption isotherm was obtained by varying the initial concentrations at room temperature.

Catalytic CO Oxidation. The catalytic oxidation of CO was conducted under atmospheric pressure in a quartz-tube fixed-bed reactor (i.d. 8 mm). A 25 mg amount of the catalyst PtNPs/CSHNFs was well mixed with quartz sand. A gas mixture of 1% CO–20% O_2–79% N_2 was passed through the catalyst bed at a flow rate of 30 mL min^{-1}. The products were analyzed by an online gas chromatograph (Shimadzu GC-8A) equipped with a TCD detector. CO conversion was calculated from the measured CO concentration using the formula CO conversion = $[(CO_{in} - CO_{out})/CO_{in}]$, where CO_{in} and CO_{out} were the inlet and outlet CO concentration, respectively.

Characterization. X-ray powder diffraction analysis was measured on a Siemens D5005 diffractometer with Cu Kα radiation (λ = 1.5418 Å). Field-emission scanning electron microscopy (FE-SEM) images were obtained with an XHITACHI S-4800 microscope. Transmission electron microscopy (TEM) and high-resolution transmission electron microscopy (HRTEM) images were obtained on a JEM-2100F microscope with an accelerating voltage of 200 kV. Inductively coupled plasma atomic emission spectroscopy (ICP-AES) analysis was performed with a TJA-POEMS spectrometer. Brunauer–Emmett–Teller (BET) surface area was measured on a Micromeritics Tristar 3000 analyzer at 77.4 K. UV–vis absorption spectra were measured at room temperature with a UV–vis–NIR (Purkinje General, TU-1900) spectrophotometer.

Conflict of Interest: The authors declare no competing financial interest.

Acknowledgment. This work was supported by the National Natural Science Foundation of China (Grant No. 21073032),

Research Fund for the Doctoral Program of Higher Education of China (No. 20120043110005), The Project Development Plan of Science and Technology of Jilin Province (20140101110JC), Opening Fund of State Key Laboratory of Inorganic Synthesis and Preparative Chemistry of Jilin University, Opening Fund of State Key Laboratory of Rare Earth Resource Utilization, Changchun Institute of Applied Chemistry, Chinese Academy of Sciences.

Supporting Information Available: Optical images, Brunauer–Emmett–Teller surface area, and EDX and TEM characterizations are given in Figures S1–S9. This material is available free of charge *via* the Internet at http://pubs.acs.org.

REFERENCES AND NOTES

1. Hu, J.; Chen, M.; Fang, X.; Wu, L. Fabrication and Application of Inorganic Hollow Spheres. *Chem. Soc. Rev.* **2011**, *40*, 5472–5491.
2. Lou, X. W.; Archer, L. A.; Yang, Z. Hollow Micro-/Nanostructures: Synthesis and Applications. *Adv. Mater.* **2008**, *20*, 3987–4019.
3. An, K.; Hyeon, T. Synthesis and Biomedical Applications of Hollow Nanostructures. *Nano Today* **2009**, *4*, 359–373.
4. Wang, Z.; Zhou, L.; Lou, X. W. Metal Oxide Hollow Nanostructures for Lithium-Ion Batteries. *Adv. Mater.* **2012**, *24*, 1903–1911.
5. Baughman, R. H.; Zakhidov, A. A.; Heer, W. A. d. Carbon Nanotubes–the Route toward Applications. *Science* **2002**, *297*, 787–792.
6. Albu, S. P.; Ghicov, A.; Macak, J. M.; Hahn, R.; Schmuki, P. Self-Organized, Free-Standing TiO_2 Nanotube Membrane for Flow-through Photocatalytic Applications. *Nano Lett.* **2007**, *7*, 1286–1289.
7. Roy, P.; Berger, S.; Schmuki, P. TiO_2 Nanotubes: Synthesis and Applications. *Angew. Chem., Int. Ed.* **2011**, *50*, 2904–2939.
8. Ding, L. X.; Wang, A. L.; Li, G. R.; Liu, Z. Q.; Zhao, W. X.; Su, C. Y.; Tong, Y. X. Porous Pt-Ni-P Composite Nanotube Arrays: Highly Electroactive and Durable Catalysts for Methanol Electrooxidation. *J. Am. Chem. Soc.* **2012**, *134*, 5730–5733.
9. Han, H.; Song, T.; Bae, J.-Y.; Nazar, L. F.; Kim, H.; Paik, U. Nitridated TiO_2 Hollow Nanofibers as an Anode Material for High Power Lithium Ion Batteries. *Energy Environ. Sci.* **2011**, *4*, 4532–4536.
10. Jayaraman, S.; Aravindan, V.; Suresh Kumar, P.; Ling, W. C.; Ramakrishna, S.; Madhavi, S. Synthesis of Porous $LiMn_2O_4$ Hollow Nanofibers by Electrospinning with Extraordinary Lithium Storage Properties. *Chem. Commun.* **2013**, *49*, 6677–6679.
11. Zhao, Y.; Jiang, L. Hollow Micro/Nanomaterials with Multilevel Interior Structures. *Adv. Mater.* **2009**, *21*, 3621–3638.
12. Qin, Y.; Liu, L.; Yang, R.; Gosele, U.; Knez, M. General Assembly Method for Linear Metal Nanoparticle Chains Embedded in Nanotubes. *Nano Lett.* **2008**, *8*, 3221–3225.
13. Ben Ishai, M.; Patolsky, F. Tube-in-Tube and Wire-in-Tube Nano Building Blocks: Towards the Realization of Multifunctional Nanoelectronic Devices. *Angew. Chem., Int. Ed.* **2009**, *48*, 8699–8702.
14. Lang, L.; Wu, D.; Xu, Z. Controllable Fabrication of TiO_2 1D-Nano/Micro Structures: Solid, Hollow, and Tube-in-Tube Fibers by Electrospinning and the Photocatalytic Performance. *Chem.—Eur. J.* **2012**, *18*, 10661–10668.
15. Wang, A. L.; Xu, H.; Feng, J. X.; Ding, L. X.; Tong, Y. X.; Li, G. R. Design of Pd/PANI/Pd Sandwich-Structured Nanotube Array Catalysts with Special Shape Effects and Synergistic Effects for Ethanol Electrooxidation. *J. Am. Chem. Soc.* **2013**, *135*, 10703–10709.
16. Zhu, Z.; Su, D.; Weinberg, G.; Jentoft, R. E.; Schlogl, R. Wet-Chemical Assembly of Carbon Tube-in-Tube Nanostructures. *Small* **2005**, *1*, 107–110.
17. Wang, Z.; Luan, D.; Li, C. M.; Su, F.; Madhavi, S.; Boey, F. Y.; Lou, X. W. Engineering Nonspherical Hollow Structures with Complex Interiors by Template-Engaged Redox Etching. *J. Am. Chem. Soc.* **2010**, *132*, 16271–16277.
18. Lou, X. W.; Yuan, C.; Archer, L. A. Shell-by-Shell Synthesis of Tin Oxide Hollow Colloids with Nanoarchitectured Walls: Cavity Size Tuning and Functionalization. *Small* **2007**, *3*, 261–265.
19. Sun, Y.; Xia, Y. Mechanistic Study on the Replacement Reaction between Silver Nanostructures and Chloroauric Acid in Aqueous Medium. *J. Am. Chem. Soc.* **2004**, *126*, 3892–3901.
20. Sun, Y.; Xia, Y. Multiple-Walled Nanotubes Made of Metals. *Adv. Mater.* **2004**, *16*, 264–268.
21. Peng, Q.; Sun, X. Y.; Spagnola, J. C.; Saquing, C.; Khan, S. A.; Spontak, R. J.; Parsons, G. N. Bi-Directional Kirkendall Effect in Coaxial Microtube Nanolaminate Assemblies Fabricated by Atomic Layer Deposition. *ACS Nano* **2009**, *3*, 546–554.
22. Mou, F.; Guan, J. G.; Shi, W.; Sun, Z.; Wang, S. Oriented Contraction: A Facile Nonequilibrium Heat-Treatment Approach for Fabrication of Maghemite Fiber-in-Tube and Tube-in-Tube Nanostructures. *Langmuir* **2010**, *26*, 15580–15585.
23. Zhang, G.; Xia, B. Y.; Xiao, C.; Yu, L.; Wang, X.; Xie, Y.; Lou, X. W. General Formation of Complex Tubular Nanostructures of Metal Oxides For the Oxygen Reduction and Lithium-Ion Batteries. *Angew. Chem., Int. Ed.* **2013**, *52*, 8643–8647.
24. Jung, J. H.; Kobayashi, H.; van Bommel, K. J.; Shinkai, S.; Shimizu, T. Creation of Novel Helical Ribbon and Double-Layered Nanotube TiO_2 Structures Using an Organogel Template. *Chem. Mater.* **2002**, *14*, 1445–1447.
25. Gu, D.; Baumgart, H.; Abdel-Fattah, T. M.; Namkoong, G. Synthesis of Nested Coaxial Multiple-Walled Nanotubes by Atomic Layer Deposition. *ACS Nano* **2010**, *4*, 753–758.
26. Zhao, Y.; Cao, X.; Jiang, L. Bio-Mimic Multichannel Microtubes by a Facile Method. *J. Am. Chem. Soc.* **2007**, *129*, 764–765.
27. Chen, H.; Wang, N.; Di, J.; Zhao, Y.; Song, Y.; Jiang, L. Nanowire-in-Microtube Structured Core/Shell Fibers *via* Multifluidic Coaxial Electrospinning. *Langmuir* **2010**, *26*, 11291–11296.
28. Liu, B.; Wei, S.; Xing, Y.; Liu, D.; Shi, Z.; Liu, X.; Sun, X.; Hou, S.; Su, Z. Complex-Surfactant-Assisted Hydrothermal Synthesis and Properties of Hierarchical Worm-like Cobalt Sulfide Microtubes Assembled by Hexagonal Nanoplates. *Chem.—Eur. J.* **2010**, *16*, 6625–6631.
29. Wang, B.; Wu, H.; Yu, L.; Xu, R.; Lim, T. T.; Lou, X. W. Template-Free Formation of Uniform Urchin-like Alpha-FeOOH Hollow Spheres with Superior Capability for Water Treatment. *Adv. Mater.* **2012**, *24*, 1111–1116.
30. Fang, Q.; Xuan, S.; Jiang, W.; Gong, X. Yolk-like Micro/Nanoparticles with Superparamagnetic Iron Oxide Cores and Hierarchical Nickel Silicate Shells. *Adv. Funct. Mater.* **2011**, *21*, 1902–1909.
31. Zhu, T.; Wu, H. B.; Wang, Y.; Rong, X.; Lou, X. W. Formation of 1D Hierarchical Structures Composed of Ni_3S_2 Nanosheets on CNTs Backbone for Supercapacitors and Photocatalytic H_2 Production. *Adv. Energy Mater.* **2012**, *2*, 1497–1502.
32. Zhu, T.; Xia, B.; Zhou, L.; Lou, X. W. Arrays of Ultrafine CuS Nanoneedles Supported on a CNT Backbone for Application in Supercapacitors. *J. Mater. Chem.* **2012**, *22*, 7851–7855.
33. Zhu, T.; Wang, Z.; Ding, S.; Chen, J. S.; Lou, X. W. Hierarchical Nickel Sulfide Hollow Spheres for High Performance Supercapacitors. *RSC Adv.* **2011**, *1*, 397–400.
34. Wang, Y.; Wang, G.; Wang, H.; Cai, W.; Zhang, L. One-Pot Synthesis of Nanotube-Based Hierarchical Copper Silicate Hollow Spheres. *Chem. Commun.* **2008**, 6555–6557.
35. Wang, X.; Zhuang, J.; Chen, J.; Zhou, K.; Li, Y. Thermally Stable Silicate Nanotubes. *Angew. Chem., Int. Ed.* **2004**, *43*, 2017–2020.
36. Wang, Y.; Tang, C.; Deng, Q.; Liang, C.; Ng, D. H.; Kwong, F. L.; Wang, H.; Cai, W.; Zhang, L.; Wang, G. A Versatile Method for Controlled Synthesis of Porous Hollow Spheres. *Langmuir* **2010**, *26*, 14830–14834.
37. Zhang, P.; Shao, C.; Zhang, Z.; Zhang, M.; Mu, J.; Guo, Z.; Liu, Y. TiO_2@Carbon Core/Shell Nanofibers: Controllable Preparation and Enhanced Visible Photocatalytic Properties. *Nanoscale* **2011**, *3*, 2943–2949.

38. Mu, J.; Shao, C.; Guo, Z.; Zhang, M.; Zhang, Z.; Zhang, P.; Chen, B.; Liu, Y. In_2O_3 Nanocubes/Carbon Nanofibers Heterostructures with High Visible Light Photocatalytic Activity. *J. Mater. Chem.* **2012**, *22*, 1786–1793.
39. Dogan, M.; Ozdemir, Y.; Alkan, M. Adsorption Kinetics and Mechanism of Cationic Methyl Violet and Methylene Blue Dyes onto Sepiolite. *Dyes Pigm.* **2007**, *75*, 701–713.
40. Wang, Y.; Wang, G.; Wang, H.; Liang, C.; Cai, W.; Zhang, L. Chemical-Template Synthesis of Micro/Nanoscale Magnesium Silicate Hollow Spheres for Waste-Water Treatment. *Chem.—Eur. J.* **2010**, *16*, 3497–3503.
41. Chen, H. M.; Lu, X. H.; Deng, C. H.; Yan, X. M. Facile Synthesis of Uniform Microspheres Composed of a Magnetite Core and Copper Silicate Nanotube Shell for Removal of Microcystins in Water. *J. Phys. Chem. C* **2009**, *113*, 21068–21073.
42. Yang, Y.; Zhuang, Y.; He, Y.; Bai, B.; Wang, X. Fine Tuning of The Dimensionality of Zinc Silicate Nanostructures and Their Application as Highly Efficient Absorbents for Toxic Metal Ions. *Nano Res.* **2010**, *3*, 581–593.
43. Ahmadi, T. S.; Wang, Z. L.; Green, T. C.; Henglein, A.; El-Sayed, M. A. Shape-Controlled Synthesis of Colloidal Platinum Nanoparticles. *Science* **1996**, 1924–1926.
44. Bratlie, K. M.; Lee, H.; Komvopoulos, K.; Yang, P.; Somorjai, G. A. Platinum Nanoparticle Shape Effects on Benzene Hydrogenation Selectivity. *Nano Lett.* **2007**, *7*, 3097–3101.
45. Takahashi, N.; Kuroda, K. Materials Design of Layered Silicates through Covalent Modification of Interlayer Surfaces. *J. Mater. Chem.* **2011**, *21*, 14336–14353.
46. Nguyen, H. L.; Nguyen, H. H.; Nguyen, D. P.; MacLaren, D. A. Co-Pt Nanoparticles Encapsulated in Carbon Cages Prepared by Sonoelectrodeposition. *Nanotechnology* **2011**, *22*, 285603.
47. Prashar, A. K.; Mayadevi, S.; Rajamohanan, P. R.; Nandini Devi, R. *In Situ* Encapsulation of Pt Nanoparticles in Mesoporous Silica: Synthesis, Characterisation and Effect of Particle Size on CO Oxidation. *Appl. Catal., A* **2011**, *403*, 91–97.
48. Zhu, J.; Wang, T.; Xu, X.; Xiao, P.; Li, J. Pt Nanoparticles Supported on SBA-15: Synthesis, Characterization and Applications in Heterogeneous Catalysis. *Appl. Catal. B: Environ.* **2013**, *130−131*, 197–217.